Available online at www.sciencedirect.com
SCIENCE DIRECT®

ELSEVIER

Journal of the European Ceramic Society 25 (2005) 1479–1486

EC≋RS

www.elsevier.com/locate/jeurceramsoc

X-ray diffraction microstructure analysis of mullite, quartz and corundum in porcelain insulators

José M. Amigó[a,*], Francisco J. Serrano[a], Marek A. Kojdecki[b], Joaquín Bastida[a], Vicente Esteve[c], María Mercedes Reventós[a], Francisco Martí[d]

[a] *Departament de Geologia, Universitat de València, 46100 Burjassot, Spain*
[b] *Instytut Matematyki i Kryptologii, Wojskowa Akademia Techniczna, 00-908 Warszawa 49, Poland*
[c] *Departament de Química Inorgànica i Orgànica, Universitat Jaume I, Ap. 224, 12080 Castelló, Spain*
[d] *Laboratorio Central, Nalda S.A., 46132 Almassera (Valencia), Spain*

Received 21 December 2003; received in revised form 24 May 2004; accepted 31 May 2004
Available online 14 August 2004

Abstract

The X-ray diffraction microstructure analysis has been performed on commercial samples of the silica and alumina porcelain insulators obtained at 1300 °C, with the same time of firing. The study was carried out on mullite, corundum and quartz by applying several integral breadth methods (i.e. the Williamson–Hall analysis, the Langford method and the Halder–Wagner approximation) and the Fourier analysis (Warren–Averbach method). The apparent crystallite sizes determined for the mullite are direction-dependent (anisotropic) and within each group of samples, on average, the greatest values are obtained along the direction [0 0 1]. With regard to the microstructure of the corundum and the quartz, there are little differences between the two groups of samples. Considering all samples on average, the crystallite sizes follow the order corundum > mullite > quartz. These microstructural data were related with the mechanical strength and with the chemical and mineralogical composition of the samples. Due to similar conditions of formation of the porcelains studied, the content of corundum seems to be the principal factor influencing their flexural strength, coinciding with small differences of crystalline microstructure.
© 2004 Elsevier Ltd. All rights reserved.

Keywords: Porcelain; X-ray methods; SiO_2; Al_2O_3; Mullite; Crystallite size; Insulators

1. Introduction

Porcelain has been used as an electrical insulating material since more than 150 years. During this long period of time it has been realised that several characteristic properties of porcelain (e.g. mechanical strength, high-power dielectric strength and corrosion resistance) as a ceramic product cannot be obtained in other materials. Today, the growing demand for porcelain in the field of electrical engineering, caused by the importance of electric energy in modern society, motivates many research projects in order to obtain the best properties for the requirements and applications of porcelain insulators. Basically, manufacturers and researchers must consider that the high-voltage porcelain insulators perform two important functions: they insulate electrically and fasten mechanically the components of the electrical distribution networks. In relation to this, the different formulations of green ceramic bodies are used in manufacturing porcelain insulators.

Two types of porcelain insulators are mostly used, the silica and alumina porcelains (classified, respectively, as C-110 and C-120 sub-groups according to IEC 672-3 standard). In general, principal differences between silica and alumina porcelains can be summarised as follows. In the silica porcelain, high temperatures or long firing time leads to a reduction of the solid quartz content in the ceramic body because of the melting of quartz grains. This reduction causes clearly the

* Corresponding author.
E-mail address: jose.m.amigo@uv.es (J.M. Amigó).

0955-2219/$ – see front matter © 2004 Elsevier Ltd. All rights reserved.
doi:10.1016/j.jeurceramsoc.2004.05.019

decrease of the mechanical strength of the porcelain; on the other hand, the differences between thermal expansion corresponding to quartz grains and the surrounding liquid phase cause mechanical stress, which can produce micro cracks in the porcelain. Intense changes of piece temperature could lead to increase the already existing micro cracks, causing reduction of mechanical strength under load. In the alumina porcelains the major portion of quartz is replaced by aluminium oxide. This leads to the increase of the mechanical strength (related to smaller number of micro cracks). During the sintering process mullite and corundum are formed and the porcelain is obtained with high content of the glass phase that leads to non-porosity but without the melting of the aluminium oxide grains (thus, high temperature or long time of firing do not affect the mechanical strength). The alumina porcelains are insensitive to temperature changes and the mechanical strength is mainly controlled by the quantity of corundum (and not by the amount of mullite as in silica porcelains).[1,2]

In a previous work,[3] a comparative study of the silica and alumina porcelain insulators was performed. The samples of commercial porcelains were analysed by the X-ray powder diffraction methods and their mineralogical and chemical compositions were related with thermomechanical properties measured in these materials. The aim of the present work is to complete that study with a microstructure analysis by the X-ray powder diffraction. It is known that the microstructure of ceramic materials has a great importance because it is related with their macroscopic properties like mechanical strength. But it is to be remembered that the microstructure has frequently a meaning associated with the grain size of different components following from microscopic observations (e.g. by scanning electron microscopy). However, the microstructure determined by the X-ray powder diffraction has a different meaning since it concerns the coherent diffraction domains, named crystallites. This X-ray diffraction (XRD) microstructure can be understood as the submicrostructure, taking into account that mineral grains are formed by a mosaic of crystallites. In the field of ceramic materials, the application of XRD microstructure analysis is not habitual for different reasons. One of them is the line overlapping, typical for ceramic materials, making an accurate treatment of line profiles corresponding to phases of interest difficult. Another problem is caused by the narrowness of some line profiles, since in these cases the extraction of microstructural information sometimes is not possible. On the other hand, the results obtained via the XRD microstructure analysis are referred to such parameters as the crystallite size (or X-ray coherence lengths) which have a physical meaning different to the grain size, frequently used for ceramic researchers. Nevertheless, in our opinion the XRD microstructure analysis offers some advantages with regard to the classic analytical methods; the sample do not need a special treatment and requires only an adequate choice of the conditions for recording the XRD powder pattern. Thus, the mineralogical analysis (qualitative and quantitative) and the microstructure analysis could be performed on the same data collected. Furthermore, the results of the XRD microstructure analysis set up statistical characteristics of the sample.

In the field of ceramic materials, the XRD microstructure analysis methods was firstly applied to study the growth of mullite crystallites in different raw materials and enabled to relate the XRD microstructure with distinctive feature of this material, the bimodality (the existence of the primary and secondary mullite), that occurs in some conditions.[4,5] In the present work, an attempt is made to obtain an explanation of principal differences between silica and alumina porcelains by taking into account the results of the XRD microstructure analysis of the samples and considering them as a complementary information to establish the connections between the XRD microstructure (crystallite parameters), the microstructure (grain parameters) and the macroscopic physical properties of technological importance (e.g. mechanical strength).

2. Experimental procedure

2.1. Material

The experiments were carried out on the commercial porcelain samples obtained from an industrial firing (at 1300 °C) of different formulae of raw materials. These samples correspond to the alumina and silica porcelains whose chemical and mineralogical contents were analysed in a previous work together with their mechanical strength[3].

Scanning electron microscopy (SEM) observations of fresh fracture of these fired porcelain insulators were made using an Hitachi S-4100 microscope at 30 kV (Fig. 1).

2.2. X-ray diffraction data collection

The porcelain samples finely crushed were split using a rotatory splitter and grounded in an agate mortar and pestle in order to break the grain microstructure containing crystallite domains. XRD data were obtained from dried material. The samples were manually pressed into standard sample holders. The powder diffraction patterns were recorded at room temperature (22 ± 2 °C) with a Bruker D5000 X-ray powder diffractometer in step-scanning mode, using Cu Kα radiation ($\lambda = 1.54178$ Å) obtained with a secondary graphite monochromator. The diffraction patterns of the samples (h line profiles) were recorded over the range 5°–90° (2θ) with the scanning step of 0.02° (2θ) and the counting time of 10 s per step. The standard line profiles for the instrumental line broadening evaluation (g) were obtained from the diffraction pattern of the standard reference material LaB_6 (SRM 660a), supplied by National Institute of Standards and Technology, and registered between 20° and 131° (2θ) using variable step lengths and times.[6,7] The goniometer was controlled by the PC software package DIFFRAC plus for Windows NT, supplied by Bruker/Socabim. Fig. 2 shows the XRD patterns corresponding to some studied samples.

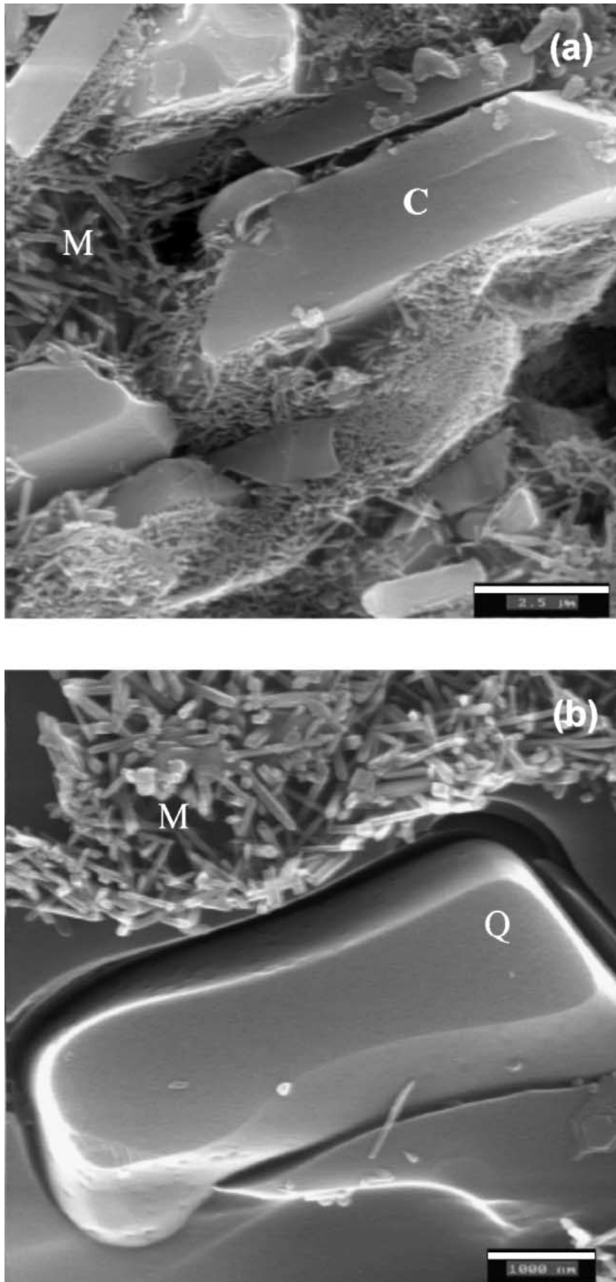

Fig. 1. SEM images: (a) S1 alumina porcelain showing corundum grains (C) and mullite needles (M) (bar = 2.5 μm), (b) S5 silica porcelain showing quartz grains (Q) and mullite needles (M) (bar = 1000 nm).

2.3. Diffraction line broadening analysis

The diffraction line broadening analysis of a crystalline phase starts with registering the XRD pattern of a sample, using the conditions good enough to obtain the reliable pure line profiles. If the sample is of a polycrystalline material, as occurs in the porcelain insulators studied in the present work, the line overlapping can be severe, making difficult or impossible an accurate analysis of some reflections. The group of reflections (h profiles) of quality enough for performing the line broadening analysis is selected and their experimental intensity distributions are adjusted to analytical functions (e.g. Voigt, pseudo-Voigt or Pearson VII) by means of the pattern-modelling software. For each adjusted line profile the following parameters are obtained: the height of the peak, I_o, the integral breadth of the line profile, β (=A/I_o, where A is the peak area) and the full-width at half-maximum intensity, FWHM (or 2ω). The same procedure is applied to the instrumental profiles (g) to obtain in this way the instrumental function giving the variation of instrumental broadening with the diffraction angle (β_g versus $^\circ 2\theta$, $2\omega_g$ versus $^\circ 2\theta$).

Two approaches are mostly used to extract microstructural data by obtaining and analysing the corrected line profiles (f): the integral breadth methods or the Fourier methods.[8] The Langford method[9,10] and the Williamson–Hall analysis[11] are within the former ones and can be considered as simplified procedures based on the assumption that the line profiles have specific shapes. Although these assumptions can be related with systematic errors, these methods are applied frequently because of their simplicity. The Fourier methods, as the Warren–Averbach analysis,[12] are more accurate procedures and therefore the requirements with regard to the amount and quality of data are greater.

In the Langford method the observed h and g profiles are assumed to be Voigtian, i.e. the convolutions of the Lorentz and Gaussian profiles. The peaks (after the filtration of only K_{α_1} component) must be symmetrical and the line-shape parameter ϕ (= $2\omega/\beta$) must lie within the Lorentzian limit (ϕ = 0.6366) and the Gaussian limit (ϕ = 0.9394). When observed β_h values are corrected for the instrumental contribution, the integral breadths of the both component, the Gaussian and the Lorentzian, of the pure profiles, β_{fG} and β_{fC}, are obtained. From β_{fG} as the data, expressed in the reciprocal space units as $\beta^*_{fG} = \beta_{fG} \cos\theta/\lambda$, the apparent crystallite size, $\varepsilon\beta = (\beta^*_{fG})^{-1}$, is calculated. If the line broadening is solely attributed to a size effect, then the apparent crystallite size is calculated using the integral breadth of the pure line profile, $\varepsilon\beta = (\beta^*_{fG})^{-1}$. In both these cases, the Scherrer formula,[13] $\beta = K\lambda/D \cos\theta$, is applied with taking the Scherrer constant K = 1. The Scherrer formula describes the mutual dependence between the line profile integral breath and the crystallite size D, which is the volume-weighted mean of the crystallite in the direction perpendicular to the diffracting planes; the constant K varies with the reflection Bragg angle and the crystallite shape.

An alternative and more easy way to obtain β_f parameter from the h profiles, corrected for the instrumental contribution, is the Halder–Wagner approximation[14,15] based on the following parabolic expression:

$$\beta_h^2 \cong \beta_f\beta_h + \beta_g^2.$$

The size parameter, ε_β, is calculated from β_f in the same way as mentioned above in the case of the Langford method.

The Williamson–Hall plot (β^*_f versus d^*) is the basis of the analysis, which is useful as the first-look estimation of

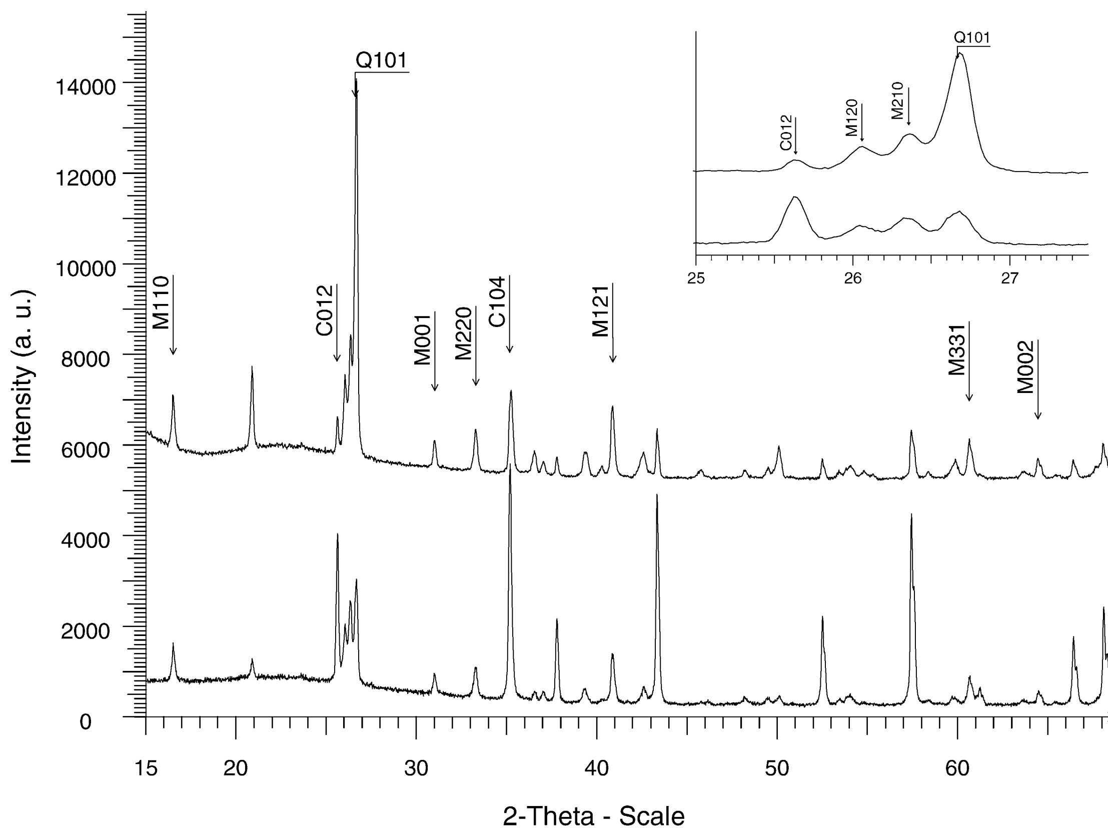

Fig. 2. XRD patterns of alumina (S4) and silica (S5) porcelains. The inset shows (enlarged) the position of the 1 2 0 and 2 1 0 reflections of the mullite.

the nature of structural imperfections present in a sample. From this plot it is possible to know if there are both the d^*-independent and d^*-dependent contributions to the line breadths. If all values of $\beta_f{}^*$ lie on a horizontal line, then the strain broadening is negligible and the crystallites are spherical on average. When the values of β_f^*, corresponding to different reflection groups, lie on several horizontal lines, the strain broadening is again negligible and the crystallite shape is not spherical. The size and strain parameters can be estimated by means of the Williamson–Hall plot, by applying the following approximate formula:

$$\beta_f^* = (\varepsilon_{WH})^{-1} + 2e_{WH}d^*,$$

where ε_{WH} is the apparent crystallite size (obtained from the intercept of the straight line β_f^* versus d^*) and e_{WH} is the strain parameter (obtained from the slope of the straight line β_f^* versus d^*). This expression assumes that all the constituent f profiles are Lorentzian. Neglecting the strain, one obtains the Scherrer formula once again.

The Warren–Averbach method[12] is based on the representation of the diffraction line profiles by means of Fourier series. This method allows to separate the broadening effects due to the crystallite size and the lattice strain, using at least two orders of the same reflection, and gives size distributions of crystallites in the sample. The size parameter obtained from Warren–Averbach method is named ε_F and has a definition different to that of ε_β. The strain parameter is defined as root-mean-square strain[10], constant or dependent on interplanar distance equal to 5 nm. This microstructural analysis has been realised using the Win–Crysize program supplied by Brucker.

In the present study the pattern decomposition for the line profile analysis was carried out by means of the Brucker/Socabim program PROFILE. All the observed XRD lines were approximated by using the pseudo-Voigt or Pearson VII function. In this way, the following lines were selected for the analysis: 1 1 0, 1 2 0, 0 0 1, 2 2 0, 2 0 1, 1 2 1, 3 3 1 and 0 0 2 (finally only 1 1 0, 2 2 0, 0 0 1 and 0 0 2) for mullite; 1 0 0, 1 0 1, 1 1 2 and 2 1 1 for quartz; 0 1 2, 1 0 4, 1 1 0, 1 1 3 and 0 2 4 for corundum.

3. Results and discussion

The set of the Williamson–Hall plots was produced for analysing the corrected line profiles corresponding to the mullite reflections from all samples (Fig. 3). Two parallel straight lines, corresponding to two pairs of the reflections of different orders (each of them corresponding to the same direction, 1 1 0–2 2 0 and 0 0 1–0 0 2), were constructed for each plot by taking the same slope of both the lines and using least-squares fitting, with good approximation. In all samples

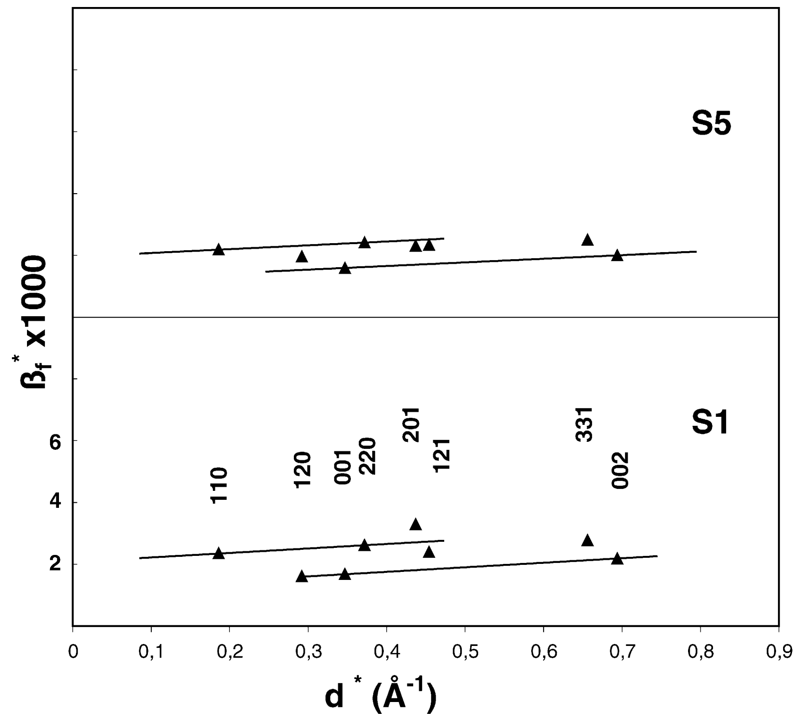

Fig. 3. Williamson–Hall plots for mullite in silica (S5) and alumina (S1) porcelains. Both the plots are presented in the same scale as applied for S1.

the anisotropy of the crystallite sizes (in different directions) are observed. These results agree with the known fact, that the growth of mullite crystallites is frequently anisotropic. The Table 1 shows the estimates of the apparent crystallite sizes and microstrains derived from these lines, mentioned above, of the Williamson–Hall plots in Fig. 3 (i.e. only for [1 1 0] and [0 0 1] crystallographic directions). Although it would be useful to study the other phases, the corundum and the quartz, in the same way to determine both the crystallite size and the microstrains, only the crystallite size were estimated for them by the Langford and Halder–Wagner methods, with neglecting the microstrains, due to the lack of sufficient number of reflections (especially those of different orders) which might be analysed. The same was done for the mullite, taking into account that the microstrains were small, as it follows from Fig. 3.

In this way, the Langford and Halder–Wagner methods were applied to all the corrected line profiles, supposing that all compounds are approximately strain-free materials; the results are showed in Table 2. The differences between the estimates of the crystallite size of the mullite in Table 1 and Table 2 are compatible with these approximations. The intercepts of the straight lines in Fig. 3, due to their slight non-zero slopes, are less than the corresponding values of the integral breadth β_f^*, what results in the crystallite size estimates in Table 1 greater than in Table 2. The discrepancies between the size estimates for the mullite obtained for the difference order of the same reflection (1 1 0 and 2 2 0 or 0 0 1 and 0 0 2, in Table 2) can be either attributed to the existence of the small microstrains, not taken into account.

It follows from the results collected in Table 1 and Table 2, that the differences in the crystallite sizes of mullite for both groups of porcelains are slightly relevant, on average. In general the crystallites in the mullite are more elongated in the direction [0 0 1] than in the direction [1 1 0]. This property is possibly consequence of the high content of the glassy phase

Table 1

Microstructural parameters obtained from the Williamson–Hall analysis for mullite in porcelain insulators (S1, S2, S3 and S4: alumina porcelains, S5, S6 and S7: silica porcelains)

Sample	[1 1 0] direction		[0 0 1] direction	
	Apparent size, ε_{WH} (nm)	Apparent strain, e_{WH}	Apparent size, ε_{WH} (nm)	Apparent strain, e_{WH}
S1	48.3	0.00298	86.2	0.00298
S2	76.3	0.00587	204.1	0.00587
S3	58.5	0.00361	133.3	0.00361
S4	40.8	0.00105	56.8	0.00105
S5	51.0	0.00240	85.5	0.00240
S6	62.5	0.00414	243.9	0.00414
S7	56.5	0.00358	158.7	0.00358

Table 2
Apparent crystallite sizes (ε_β expressed in nm) for mullite, M; corundum, C and quartz, Q in porcelain insulators (LM: Langford method, H–W: Halder–Wagner approximation)

hkl	Alumina porcelains								Silica porcelains					
	S1		S2		S3		S4		S5		S6		S7	
	LM	H–W	LM	H–W	LM	H–W	LM	H–W	LM	H–W	LM	H–W	LM	H–W
M														
1 1 0	43.5	44.6	52.9	58.4	52.3	57.4	37.7	38.3	46.8	49.4	50.0	52.0	50.2	55.0
0 0 1	58.6	55.8	67.6	66.0	69.3	74.3	–[a]	52.9	62.3	61.8	89.1	86.4	76.1	74.3
2 2 0	37.3	37.6	42.4	43.2	39.6	40.1	39.3	40.1	40.8	41.7	42.6	43.2	39.2	39.7
0 0 2	46.6	45.9	39.2	37.4	51.5	51.1	46.0	43.3	50.6	48.7	53.7	50.5	55.1	53.8
C														
0 1 2	93.0	98.9	103.2	107.8	110.9	115.8	64.9	68.9	–[a]	86.8	123.7	144.1	94.3	103.4
1 0 4	67.9	63.8	67.4	66.5	100.6	109.3	52.9	53.0	99.0	104.5	40.5	41.5	87.4	93.6
1 1 0	81.2	86.6	83.0	86.6	87.2	95.5	64.8	66.5	–[a]	63.3	90.7	91.9	–[a]	74.0
1 1 3	77.6	81.2	82.1	86.7	82.5	86.7	73.0	77.2	77.5	81.2	80.1	83.8	76.0	79.6
0 2 4	73.6	75.8	72.0	73.8	75.0	77.2	66.5	66.6	72.7	74.4	70.1	71.2	73.8	75.8
Q														
1 0 0	48.8	47.3	52.3	52.7	–[a]	46.5	–[a]	40.3	53.8	57.3	56.1	54.5	51.0	50.0
1 0 1	65.0	70.1	68.1	75.0	57.6	62.2	49.6	52.3	57.4	62.2	54.5	58.4	57.5	60.7
1 1 2	35.8	36.1	34.7	34.3	32.9	32.8	–[a]	33.0	34.4	34.7	30.0	30.2	30.0	30.2

[a] In these cases the Langford method failed.

in porcelains. It is known that the glassy phase facilitates the mass transport in solid-state reactions and would accelerate the crystallite growth, especially in the preferable direction [0 0 1]. The morphology of mullite grains observed by SEM (Fig. 1) seems to agree with these results.

The crystallite size values obtained by means of the Langford method and the Halder–Wagner approximation (Table 2) have been compared in order to reveal if there exists any systematic difference between the results from the two procedures used. The good correlation between both sets of numbers (Fig. 4) shows that it is not the case. It can be noticed, that in several cases the Langford method failed to calculate the pure line profiles f from the pairs of peaks *h* and *g* with integral breadth of Gaussian or Lorentzian part of *g* greater than that of h. The Halder–Wagner approximation was still applicable in these cases.

Results from Table 2 show that the corundum is the mineral phase of the greatest crystallite size values ($\varepsilon_\beta > 70$ nm) while quartz and mullite have smaller crystallite sizes. In order to visualize the possible differences between the crystallite sizes of both groups of samples, an average value has been calculated for each phase (Fig. 5). In this way it is possible to consider if the different mechanical properties of both alumina and silica porcelains[3] can be related with microstructural parameters. The crystallite sizes of quartz and corundum what can be seen in Fig. 5 are very similar in both groups and therefore no influence of their XRD microstructure could be attributed to mechanical strength differences

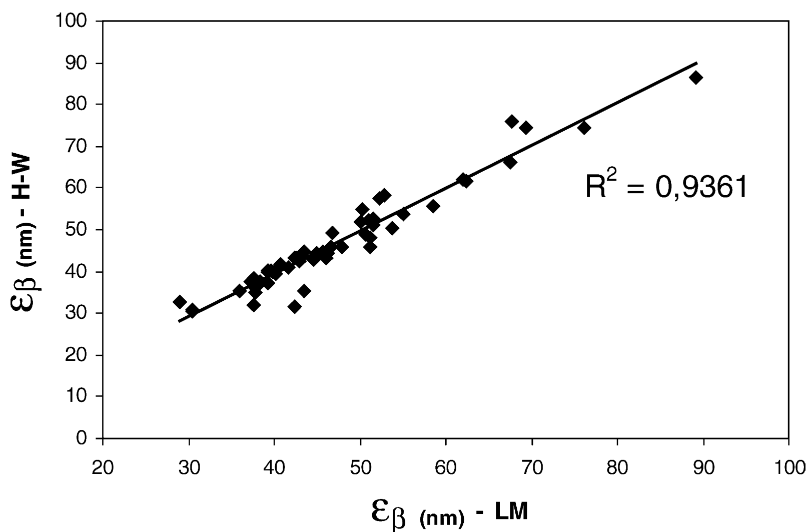

Fig. 4. Correlation between crystallite sizes of mullite obtained in silica and alumina porcelains using Langford method and Halder–Wagner approximation (Results from the following lines are considered: 1 1 0, 1 2 0, 0 0 1, 2 2 0, 2 0 1, 1 2 1, 3 3 1 and 0 0 2).

Table 3
Microstructural parameters obtained by Warren–Averbach analysis for mullite in porcelain insulators

Sample	*hkl*	Size, ε_F (nm)	RMS strain ($L = 5$ nm)
Alumina porcelains			
S1	1 1 0–2 2 0	43.4	0.00247
	0 0 1–0 0 2	48.0	0.00155
S2	1 1 0–2 2 0	43.0	0.00278
	0 0 1–0 0 2	86.8	0.00227
S3	1 1 0–2 2 0	33.5	0.00000
	0 0 1–0 0 2	85.8	0.00088
S4	1 1 0–2 2 0	34.6	0.00237
	0 0 1–0 0 2	29.3	0.00000
Silica porcelains			
S5	1 1 0–2 2 0	42.3	0.00281
	0 0 1–0 0 2	38.7	0.00000
S6	1 1 0–2 2 0	34.7	0.00213
	0 0 1–0 0 2	85.6	0.00141
S7	1 1 0–2 2 0	36.3	0.00290
	0 0 1–0 0 2	48.5	0.00000

between alumina and silica porcelains. On the other hand, a little bigger crystallite sizes of mullite corresponding to silica porcelains do not seem to have a positive effect on the mechanical strength, as can be verified taking into account average values of both magnitudes. The differences between the mechanical properties of both groups of samples should rather be related to larger corundum content in the alumina porcelains (on average, 34.4% versus 8.7%).

The same set of samples submitted to integral breadth methods was analysed by means of the Warren–Averbach method (Table 3). In a previous work[5] this method was used in order to evaluate crystallite size distributions of mullite corresponding to fired samples of kaolinite–alumina mixtures. Only crystallite size distributions along the direction [1 1 0] were measured and the results were related to the presence of primary (elongated grains) and secondary mullite (equiaxed grains) in the samples. This bimodal crystallite size distribution was detected through two maximums of relative frequency. In the present work the application of the Warren–Averbach method has been performed considering furthermore the crystallographic direction [0 0 1]. At the first glance, the results show in all porcelains only one maximum for the crystallite size distribution curve corresponding to [1 1 0] direction. Nevertheless, surprisingly, the data for [0 0 1] direction give a bimodal distribution curve with two maximums of relative frequency slightly more accentuated in the alumina porcelains (Fig. 6). Taking into account that the quickest rate of growth of mullite crystallites has been observed along the [0 0 1] direction[4], an interpretation of these results could be as follows: At a temperature of 1300 °C the quantity of secondary mullite present in the porcelain samples must be very low. Accordingly, the SEM micrographs of the samples do not show evidence of a bimodal morphology in the mullite grains. However, the distribution curve for the [0 0 1] direction suggest that the process of secondary formation has been initiated. Assuming this hypothesis, we can conclude that the observation of two fractions of mullite crystallites corresponding to this early stage can be made only in the nanometric scale, by means of XRD microstructural analysis methods. In our opinion, higher temperatures of firing would origin the subsequent development of secondary mullite, giving as a result a crystallite size distribution curve for the [1 1 0] showing also two maximums of relative frequency.

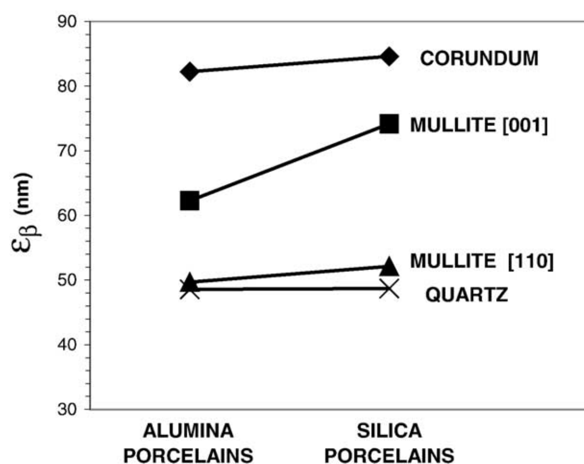

Fig. 5. Average crystallite sizes for corundum, quartz and mullite in alumina and silica porcelains determined by means of Halder–Wagner approximation (corundum: average values for all studied lines, quartz: average values for 1 0 0, 1 0 1, and 1 1 2 lines, mullite [1 1 0]: average values for 1 1 0 line, mullite [0 0 1]: average values for 0 0 1 line).

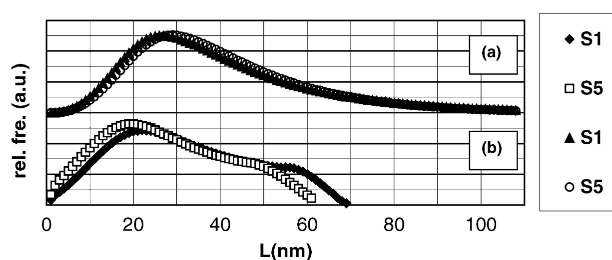

Fig. 6. Relative frequency of crystallite sizes distribution using a Pearson VII function for mullite in alumina (S1) and silica (S5) porcelains: (a) along [1 1 0] direction and (b) along [0 0 1] direction.

4. Conclusions

The two groups of porcelain insulators analysed in this work have different macroscopic characteristics influenced mainly by their chemical and mineralogical compositions. This fact, considered as the point of departure of this investigation, has been studied from the viewpoint of the crystallite size parameters obtained by the XRD microstructure analysis of mullite, corundum and quartz.

In general, the differences between the crystallite sizes of each specific phase are small. However, when an average value is calculated for each group of samples, we can verify the following results:

(1) The microstructural analysis by means of XRD allows detecting the formation of secondary mullite, whose con-

tent present in the porcelain samples should be low. These crystallites of nanometric scale are invisible in a textural study realized only by SEM microscopy.

(2) The average crystallite sizes for corundum and quartz are similar in the two groups of samples and seem to not depend on the mass content of each of these mineral phases.

(3) The crystallite sizes of mullite are, on average, very similar for both groups of porcelains and show relevant differences between the directions of growth (the greatest values are obtained for the [0 0 1] direction).

(4) In general the crystalline microstructure of the samples analysed has no evident relation to their mechanical strength, which seems to be influenced principally by the content of corundum.

(5) Although a slight dependence of the mean crystallite sizes on mineral composition of sample can be noted, the accuracy of the methods applied for the microstructure analysis is insufficient to characterise the differences quantitatively. The XRD microstructure is influenced first of all by the conditions of the heat treatment (time and temperature), the same for all samples.

(6) The results of the average length using Warren–Averbach method for mullite usually verify crystallite sizes evaluated from the Scherrer equation (simplified integral breadth methods). The results of the Warren–Averbach analysis suggest that these porcelains consists of two different kinds of crystallites, characterized by quite different mean sizes; this is very clear in alumina porcelains in the [0 0 1] direction. It appears also in silica porcelains though slightly less marked. In both kinds of porcelains mean sizes in the [1 1 0] direction are smaller than those measured in the [0 0 1] direction.

The present study on silica and alumina porcelain insulators obtained at 1300 °C, with the same time of firing, has showed that the microstructural properties, at the nanometer scale, by X-ray powder diffraction can be used in ceramic applications with a reasonable precision. In the authors' opinion, such analyses should be applied more often when studying nanocrystalline materials and should complement the evaluation by an scanning electronic microscopy study that gives, to micrometric scale, particle sizes, whereas an X-ray diffraction study detect crystallite sizes, down to 100 nm, more related to structural properties.

Acknowledgements

The authors wish to thank Prof. Daniel Louër and to one anonymous reviewer for his helpful criticisms and suggestions. The financial support from the Spanish Department of Education (D.G.U. No. SB2001-0088) for the stay of M. A. K. in the University of Valence is gratefully acknowledged. This research was supported by a OCYT-Generalitat Valenciana project (No. GV01-527).

References

1. Liebermann, J., The standard and trend for alumina porcelain insulators. *Cfi-Ceram. Forum Int.*, 2000, **77**(6), 17–23.
2. Liebermann, J., Reliability of materials for high voltage insulators. *Am. Ceram. Soc. Bull.*, 2000, **79**(5), 55–58.
3. Amigó, J. M., Clausell, J. V., Esteve, V., Delgado, J. M., Reventós, M. M., Ochando, L. E. *et al.*, X-ray powder diffraction phase analysis and thermomechanical properties of silica and alumina porcelains. *J. Eur. Ceram. Soc.*, 2004, **24**, 75–81.
4. Serrano, F. J., Bastida, J., Amigó, J. M. and Sanz, A., XRD line broadening studies on mullite. *Crystal Res. Technol.*, 1996, **31**, 1085–1093.
5. Sainz, M. A., Serrano, F. J., Amigó, J. M., Bastida, J. and Caballero, A., XRD microstructural analysis of mullites obtained from kaolinite-alumina mixtures. *J. Eur. Ceram. Soc.*, 2000, **20**, 403–412.
6. Cline J. P., Deslattes R. D., Staudenmann J.-L., Hudson L. T., Henins A. and Cheary R. W., NIST Certificate, SRM 660a Line position and line shape standard for powder diffraction. NIST, Gaithersburg, MD, 2000, pp. 1–4.
7. Audebrand, N., Auffrédic, J.-P. and Louër, D., X-ray diffraction study of the early stages of the growth of nanoscale zinc oxide crystallites obtained from thermal decomposition of four precursors. General concepts on precursor-dependent microstructural properties. *Chem. Mater.*, 1998, **10**, 2450–2461.
8. Louër, D. and Audebrand, N., Profile fitting and diffraction line-broadening analysis. *Adv. X-ray Anal.*, 1999, **41**, 556–565.
9. Langford, J. I., A rapid method for analysing breadths of diffraction and spectral lines using the Voigt function. *J. Appl. Crystallogr.*, 1978, **11**, 10–14.
10. Langford J. I., Use of pattern decomposition or simulation to study microstructure: theoretical considerations. In *Defect and microstructure analysis by diffraction, IUCr Monographs on Crystallography 10*, ed. R. Snyder, J. Fiala and H. J. Bunge. International Union of Crystallography—Oxford Science Publications, New York, 1999, pp. 59–81.
11. Williamson, G. K. and Hall, W. H., X-ray line broadening from filed aluminum and wolfram. *Acta Metallurg.*, 1953, **1**, 22–31.
12. Warren, B. E. and Averbach, B. L., The effect of cold-work distortion on X-ray patterns. *J. Appl. Phys.*, 1950, **21**, 595–599.
13. Scherrer, P., Bestimmung der Grösse und der inneren Struktur von Kolloidteilchen mittels Röntgenstrahlung. *Nachr. Ges. Wiss. Göttingen*, 1918, **2**, 98–100.
14. Halder, N. C. and Wagner, C. N. J., Separation of particle size and lattice strain in integral breadth measurements. *Acta Crystallogr.*, 1966, **20**, 312–313.
15. Halder, N. C. and Wagner, C. N. J., Analysis of the broadening of powder pattern peaks using variance, integral breadth, and Fourier coefficients of the line profile. *Adv. X-ray Anal.*, 1966, **6**, 91–110.